ADVANCED ELECTRONIC MATERIALS
www.advelectronicmat.de

Releasable High-Performance GaAs Schottky Diodes for Gigahertz Operation of Flexible Bridge Rectifier

*Yei Hwan Jung, Huilong Zhang, In-Kyu Lee, Joo Hwan Shin, Tae-il Kim, and Zhenqiang Ma**

Novel strategies for printed electronic devices have rapidly evolved, particularly using thin films of inorganic semiconductors for high-performance. As one of the basic electronic components, diodes provide important functionalities in circuits, such as high-frequency switching and rectifying. In this report, the fabrication of releasable radio frequency (RF) gallium arsenide (GaAs)-based Schottky diodes is presented. This technique yields thousands of fully formed diodes with uniform performance densely packed onto a wafer piece, where each diode is released and transferred using a micro-stamp only when needed. Such production technique not only reduces material cost, but also benefits design efforts, as circuit designing often requires iterative designs with incremental changes. With low forward voltage and fast switching action, these printable forms of Schottky diodes are operable at microwave frequencies for diverse circuit applications. A full wave bridge rectifier, popularly used for RF-to-direct current (DC) converting circuit in wireless power transmission, is fabricated on a flexible substrate using four printed Schottky diodes. The results reveal successful RF-to-DC conversion with efficiency of up to 36.4% at principle frequency bands of mobile electronics, including cellular networks, Bluetooth, and Wi-Fi. The methods presented in this work form a simple yet robust path toward advanced high-performance flexible electronics.

Exploiting reliable fabrication technology for printable devices with high performance is the key to successful advancement of flexible and stretchable electronics.[1–4] Although advanced device engineering using transfer printing of thin-film materials has led to significant progress in performance and reliability, limitations such as sophisticated design and fabrication processes remain as drawbacks. For circuit designers, it is essential that performances of electronic devices remain uniform over multiple iterations of fabrication, due to frequent redesigning and impedance matching.[5,6] In many printed electronics fabrication procedures, semiconductor materials are printed on the target substrate followed by device fabrication. Post-transfer printing fabrication procedures on foreign substrates typically include ohmic contact formations, dielectric depositions, semiconductor etchings, etc.[1,7,8] Due to a much lower melting point of most flexible substrates compared with rigid semiconductor substrates, high-temperature processes like thermal annealing and ion implantation are generally incompatible in post-transfer printing procedures, limiting the performance of flexible electronics. Moreover, despite following the same process recipes and conditions, such post-processing on foreign substrates may lead to variations in performances between the devices fabricated separately. Minor changes in the performance can lead to impedance matching catastrophes in radio frequency (RF) engineering, as engineers rely on electrical properties obtained from a previous batch to precisely redesign the following batch. This challenge can be solved with deterministic assembly transfer printing technique utilizing releasable fully formed devices, where microfabrication processes are performed at the wafer level, with the post-transfer process only including final metallization of the devices on the foreign substrate.[9–11] Fabrication using such method can produce a large array of devices with uniform performance parameters in a single batch, leading to flexibility in designing various integrated circuits and to reducing semiconductor materials cost. Furthermore, upon depletion of all devices, the host substrate is available for regrowth of the active layers and subsequent fabrication of releasable devices.

While diverse printable fully formed transistors were developed, diodes, which act as check valves in all electronic circuits for modulation and detection of signals, were often overlooked in printed electronics development. For practical applications, diodes must operate at high switching speeds comparable to transmission frequencies of other high-speed components. Numerous flexible diode designs using novel materials, such as organic polymers, nanoparticles, or amorphous thin films, have demonstrated exceeding performance characteristics, but

Dr. Y. H. Jung, J. H. Shin, Prof. T.-i. Kim
School of Chemical Engineering
Sungkyunkwan University (SKKU)
Suwon 16419, Republic of Korea
Dr. Y. H. Jung, H. Zhang, I.-K. Lee, Prof. Z. Ma
Department of Electrical and Computer Engineering
University of Wisconsin-Madison
Madison, WI 53706, USA
E-mail: mazq@engr.wisc.edu

The ORCID identification number(s) for the author(s) of this article can be found under https://doi.org/10.1002/aelm.201800772.

DOI: 10.1002/aelm.201800772

require modified fabrication processes that may be incompatible with existing electronics or too complex and/or expensive.[12–18] A low cost and generally process-compatible method using conventional semiconductors would be more attractive in such simple device fabrications. Flexible diodes using single-crystalline nanomembrane materials were groundbreaking towards this goal, but followed post-transfer device fabrication methods that might lead to performance inconsistencies.[19,20]

Because the electrical properties of semiconductor devices depend heavily on the material properties of the semiconductor, we have utilized superior characteristics of compound semiconductors to fabricate high-performance electronics in printed formats. High-performance devices based on compound semiconductors (primarily III–V) were employed in various classes of printed electronics, including electronic, optoelectronic, photonic devices, and integrated circuits.[2,3,21–24] Especially, the mobility benefits and fabrication developments of III–V compound semiconductors allowed for both analog and digital circuits operating at microwave frequencies and high speeds. For high-frequency applications, including mobile communications electronics, gallium arsenide (GaAs) provides superior electrical characteristics over silicon (Si).[25,26] For instance, GaAs possesses electron mobility that is six times greater than Si and significantly better noise performance. These two key criteria are coincidentally required for RF electronics. Thus, using printed forms of GaAs for future wearable and implantable technology with mobile communication capabilities is inevitable. However, III–V compound semiconductors like GaAs can be many times more expensive than Si or other counterparts, due to the sophisticated method by which the epitaxial layers are grown.

In this report, a low-cost production method of manufacturing fully formed printable Schottky diodes using high-performance GaAs is presented. We introduce materials and device designs that allow deterministic assembly and integration processes to benefit two important aspects of printed electronics fabrication: cost and performance uniformity. The releasable set of diodes in a densely configured host wafer presented here can be individually picked up only when required, for efficient utilization of the material. As a result, thousands of fully formed high-performance and high-frequency GaAs Schottky diodes with uniform electrical properties were achieved. To show circuit integration potential of the approach, we fabricated a full wave bridge rectifier using randomly selected four printed diodes and demonstrated efficient conversion of multi-gigahertz RF signals to direct current (DC) output on a flexible substrate. This marks the first demonstration of a flexible microwave bridge circuit as well as a flexible rectifier capable of harvesting signals at super high-frequency (SHF; beyond 3 GHz) band, an International Telecommunication Union (ITU)-designated band used for radar transmitters and wireless local area network (WLAN).

Figure 1 describes the detailed procedure for fabricating releasable GaAs-based Schottky diodes using schematic illustrations. Epitaxial layers of lightly doped n^- GaAs (600 nm) and heavily doped n^+ GaAs (1000 nm) were grown on a 500 nm thick aluminum arsenide (AlAs)-based sacrificial layer on a GaAs wafer. Ohmic and Schottky metal contacts were formed with conventional microfabrication techniques used for making high-performance GaAs devices.[27] Transmission line model-based optimization revealed that palladium and germanium alloy formed high-quality ohmic contacts on our diodes, with a specific contact resistance of 3.97×10^{-6} Ω cm^2 (Figure S1, Supporting Information). Deep mesa-etching process isolated the devices and completed the fully formed diode fabrication. After this process, AlAs layer remained beneath each diode, as shown in Figure 1a,b. A significant feature of releasable devices is to have all the devices tethered to the host wafer after removing the sacrificial layer to allow individual transfer of devices when needed. Micro-scale anchors provide just enough structural stability during storage, while breaking with fracture upon external contact, such as a grasp using a micro-stamp. Such releasable devices have been demonstrated using diverse anchor mechanisms, including underneath photoresist border, photoresist bridge, thin-film material bridge, and structured elastomers.[10,11,21,28–33] For this study, we utilized the photoresist bridge method, which fully covers the surface of the device (Figure 1c). Surface passivation is essential for GaAs-based electronics to suppress arising dangling bonds from native oxide formation, especially for long-term reliability.[26] After removal of the sacrificial layer, the diodes were freestanding and held only by the photoresist-based protective anchors, allowing the devices to be tethered to the host wafer before transfer (Figure 1d). Four anchor bridges, each with 5 μm width, held a single diode. Releasing a single fully formed diode from the host substrate requires an elastomer stamp that matches its physical dimensions to the diode dimensions. This stamp was prepared using polydimethylsiloxane (PDMS) elastomer via a micro-molding process. Van der Waals contact with the soft elastomer stamp to the device broke the anchors on all four bridges and easily picked up a single device upon retraction (Figure 1e), followed by transfer printing onto a foreign substrate, such as polyimide (Figure 1f). This process can be achieved in a precisely controlled manner using a modified mask aligner. After removing the photoresist anchor, a polyimide encapsulation layer was spin-casted to prevent the diode from oxidation. The device was completed with via-holes opening, followed by a final metallization process (Figure 1g).

Figure 2a shows the array of GaAs-based Schottky diodes ready for pick-up. On a small piece (5×6 mm^2) of GaAs wafer, a total of 1200 densely arrayed Schottky diodes with high yield were fabricated. Figure 2b shows the magnified optical image of a set of diodes. The photoresist covers the entire diode with four bridges holding the device to the larger photoresist pads that are tethered to the host substrate. The photoresist anchor not only tethers the device to the substrate, but also protects the device by covering most of the surface area, thereby increasing the storage lifetime of the diodes, as shown in the close-up view of a single diode in Figure 2c. Figure S2 (Supporting Information) shows optical images of the host GaAs wafer after pick-up and the backside of the device on PDMS micro-stamp. Hydrofluoric acid (HF)-based etching formed aluminum fluoride residues on both surfaces. Such non-volatile residues only form in extremely low quantities[22] and HF-based GaAs release techniques have been demonstrated to have negligible effects on the device performance.[2,21] Different epitaxial sacrificial layers and release etchants may be substituted for epitaxial lift-off process.[22] With the device attached temporarily to the PDMS stamp, this device can be printed onto nearly any type of adhesive coated foreign substrates. For demonstration, a

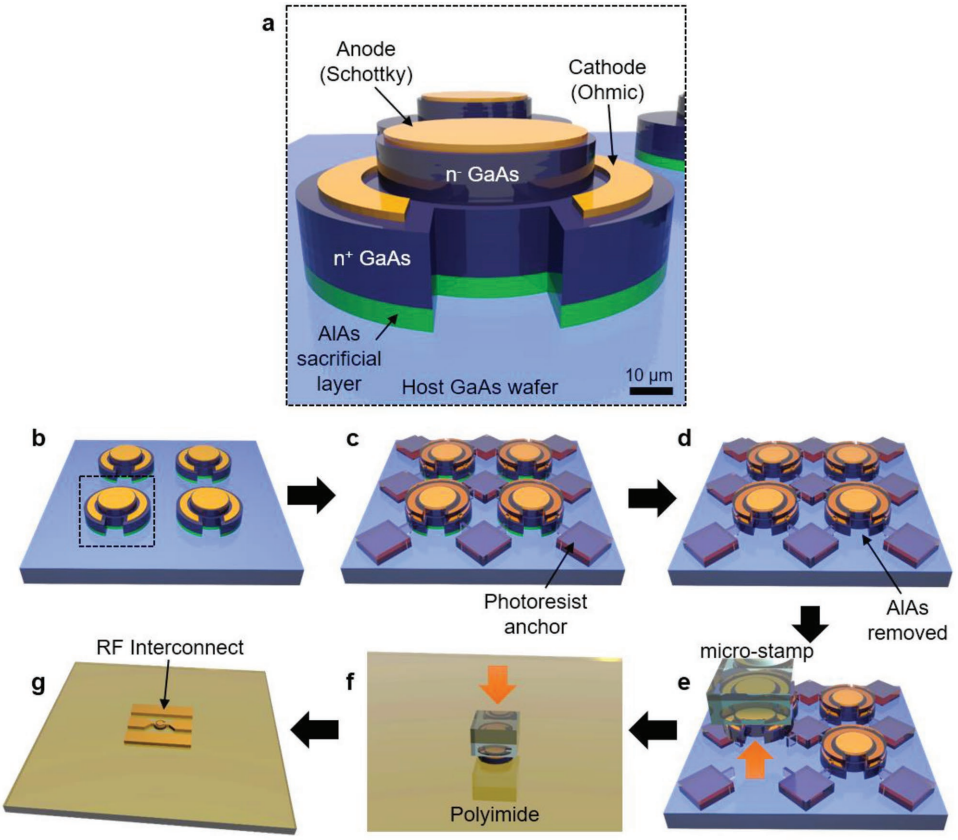

Figure 1. Schematic illustration of the fabrication process of releasable fully formed GaAs Schottky diodes. a) Structure of the GaAs Schottky diode. b) A dense array of Schottky diodes is fabricated on a sacrificial layer grown on a GaAs substrate using high-temperature processes. c) Protective anchors and temporary micro-bridges made of photoresists are formed on top of each diode. d) The AlAs sacrificial layer beneath the diodes is removed with wet etchant. e) A diode is picked up using an elastomer micro-stamp from the host wafer. f) The diode is released onto the flexible polyimide substrate using partially cured polyimide layer as an adhesive. g) Photoresist anchor is removed, followed by full curing of polyimide and RF interconnect deposition.

diode was picked up and printed onto a polyimide substrate, as shown in Figure 2d. Figure 2e,f shows the optical images of the device with RF interconnect deposited on the device for measurements. As such, deterministic assembly of the diodes can easily be achieved by mounting the micro-stamp on the modified mask aligner and repeating the pick-up and printing process, followed by passivation and metallization.

Dimensions of the releasable Schottky diodes were optimized for high-performance and to increase the yield of release and pick-up process. Schottky diodes with variable distance between the anode and the cathode were fabricated and characterized (Figure S3, Supporting Information). Four different devices with varying anode–cathode distances (d = 10, 8, 6, 4 μm) were fabricated and measured on wafer. It was observed that the DC performance remained relatively constant under forward bias with varying distances. The extracted ideality factor at forward bias of 0.1 V for the diodes with distances of 10, 8, 6, and 4 μm was 1.044, 1.037, 1.046, and 1.037, respectively. Magnifying the reverse bias performance (Figure S3d, Supporting Information), a slight decrease in OFF current was observed as the distance was decreased. This is attributed to the lower surface recombination resulting from the smaller surface area of the diode. Generally, a smaller distance between the anode and cathode leads to a smaller series resistance, thereby increasing the RF performance of the diode; nevertheless, the distance should be large enough to maintain low parasitic capacitance, which also affects RF performance. Also, for optimal RF performance under reverse bias, the anode area should be kept small to decrease junction capacitance, which is especially important for millimeter wave applications. However, the design of the releasable Schottky diode is also affected by the fabrication process. For instance, HF slowly etches GaAs through the porous photoresist protection anchor during the AlAs sacrificial layer etching process, limiting the sizes of the metal contacts. Experimenting with smaller metal contacts, the 3 h HF-based etching process eventually lifted off the metal anodes. A larger cathode area leads to a larger area of the fragile thinner region (n^+ GaAs) of the thin-film device. This induced a larger stress upon release, where a slight mechanical force from the micro-stamp caused cracks along the n^-/n^+ GaAs junction. The final dimensions of the releasable Schottky diode were chosen such that the radius of the circular anode metal is 25 μm, and the distance between cathode and anode is 4 μm. Furthermore, the thickness of the GaAs epitaxial layers can affect the performance of the diodes, as the distance from the edge of the depletion region to the ohmic contact induces series impedance.[34] The thickness of highly doped (n^+) layer is negligible in our structure because the ohmic contact is formed on top and

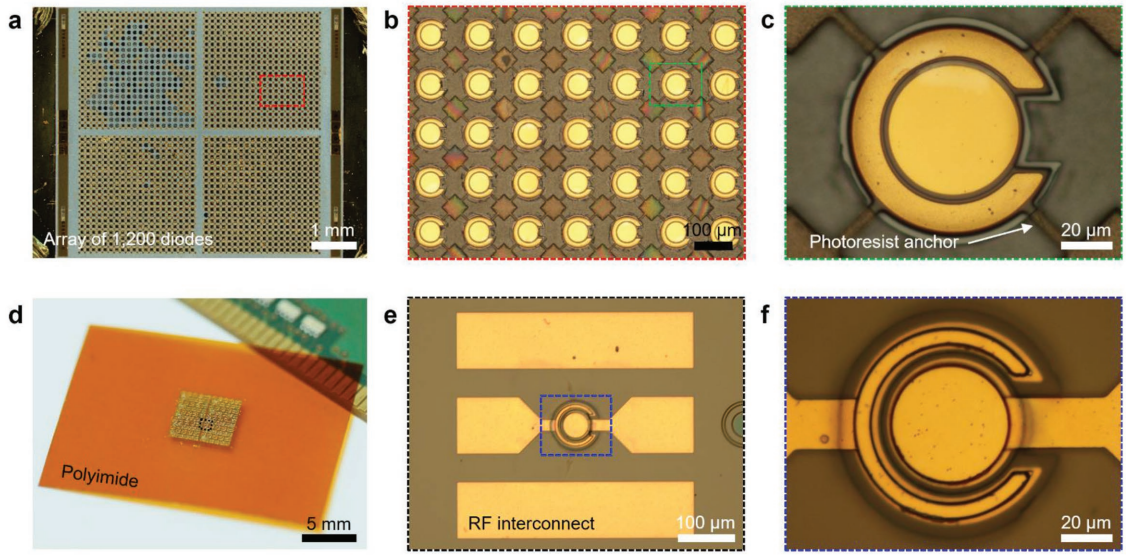

Figure 2. Optical microscopy images showing the GaAs-based Schottky diodes. a) Image of an array of 1200 releasable Schottky diodes tethered to the host GaAs wafer, ready to be picked up. b) Magnified image of the wafer in (a), showing 35 Schottky diodes. c) Magnified image of a single Schottky diode. The diode is held by four photoresist-based anchor bridges, each with a width of 5 µm, to the host GaAs wafer. d) Photograph image of an array of Schottky diodes printed onto a polyimide substrate, passivated and metalized for measurement. e) Image of a single Schottky diode showing RF interconnect. f) Magnified image of the diode in (e).

impedance is rather dominated by the anode–cathode distance, as explained above. Thinner low-doped (n^-) layer generally reduces series resistance, which benefits high-frequency operation, but it should be sufficiently thick to allow high breakdown voltage. Fabricating releasable GaAs-based nanomembranes (sub-micron) results in wavy lateral structures during release and ultimately results in crack formations during the pick-up process, due to the brittle instability of GaAs at the nanometer scale. While thicker membrane may also result in cracks, isolation of individual devices increases the structural stability at microscale thickness, preventing crack formations during the pick-up process. Thus, our epitaxial layers were chosen to enhance release and pick-up yield, by utilizing overall layer thickness of over 1 µm. The following DC and RF performance analysis of the printed Schottky diode on polyimide substrate shows that this diode is suitable for microwave frequency applications.

DC and RF performances of the printed diode on flexible polyimide substrate were characterized. An array of Schottky diodes transferred onto flexible polyimide is shown in **Figure 3**a. An ideal Schottky diode with a low turn-on voltage of 0.7 V was observed and a good ideality factor of 1.073 at forward bias of 0.5 V was extracted from the logarithmic plot presented in Figure 3b. The current ON/OFF ratio could reach over 10^7 with bias from –0.5 to 0.9 V. The consistency of the diodes can be observed from the comparison curves of eight Schottky diodes that were individually transferred onto different polyimide substrates presented in Figure 3c. At a forward current bias of 10 mA, voltage ranged from 0.96 to 1.03 V (inset of Figure 3c). A slight shift in the current–voltage curve of the flexible Schottky diode was observed under extreme bent condition (radius of curvature, $r = 2$ mm), as presented in Figure 3d. This is attributed to the change of Schottky barrier height under strain.[35] Over 100 cycles of bending to a radius of curvature of 5 mm, the voltage measured at flat states ranged from 0.99 to 1.08 V (inset of Figure 3d). Figure 3e,f presents the measured S-parameters of the diode at forward bias and reverse bias, respectively. At a forward current bias of 10 mA, the insertion loss (S_{21}) was only –0.572 dB at 2.4 GHz and –0.979 dB at 50 GHz. At a reverse voltage bias of 0.5 V, the insertion loss (S_{21}) reached –4.211 dB at 2.4 GHz and –2 dB at 4.03 GHz. The low insertion loss at forward bias and high insertion loss at reverse bias enable the flexible Schottky diode as an RF switch for wireless communication at gigahertz frequencies. An embedded junction field effect transistor (JFET) model in Keysight Advanced Design System (ADS) was employed to simulate the RF characteristics of the diode with source and drain connected. The simulated S-parameters shown in Figure 3e,f fit well with the measured results at forward and reverse bias.

Printed integrated circuits requiring multiple diodes with consistent electrical performance can be built using the fully formed releasable diodes presented in this report. One of the high-performance and high-frequency electronic circuits that require multiple diodes with uniform performance parameters is the diode bridge, where four or more equivalent diodes are arranged in a bridge circuit to provide the same polarity of output for either polarity of input. To evaluate the practicality and the high-frequency operating capability of our devices, a full wave bridge rectifier consisting of four printed Schottky diodes was fabricated on a polyimide substrate. **Figure 4**a shows the circuit diagram of the RF-to-DC rectifier designed to operate at popular mobile electronics operating frequencies, such as mobile network, Bluetooth, and Wi-Fi. Fabrication of the rectifier involved printing of the four diodes that were individually transferred from the host wafer using the deterministic transfer printing approach, followed by depositions of metal contacts and metal–insulator–metal (MIM) capacitors. An optical microscopy image of the completed rectifier is

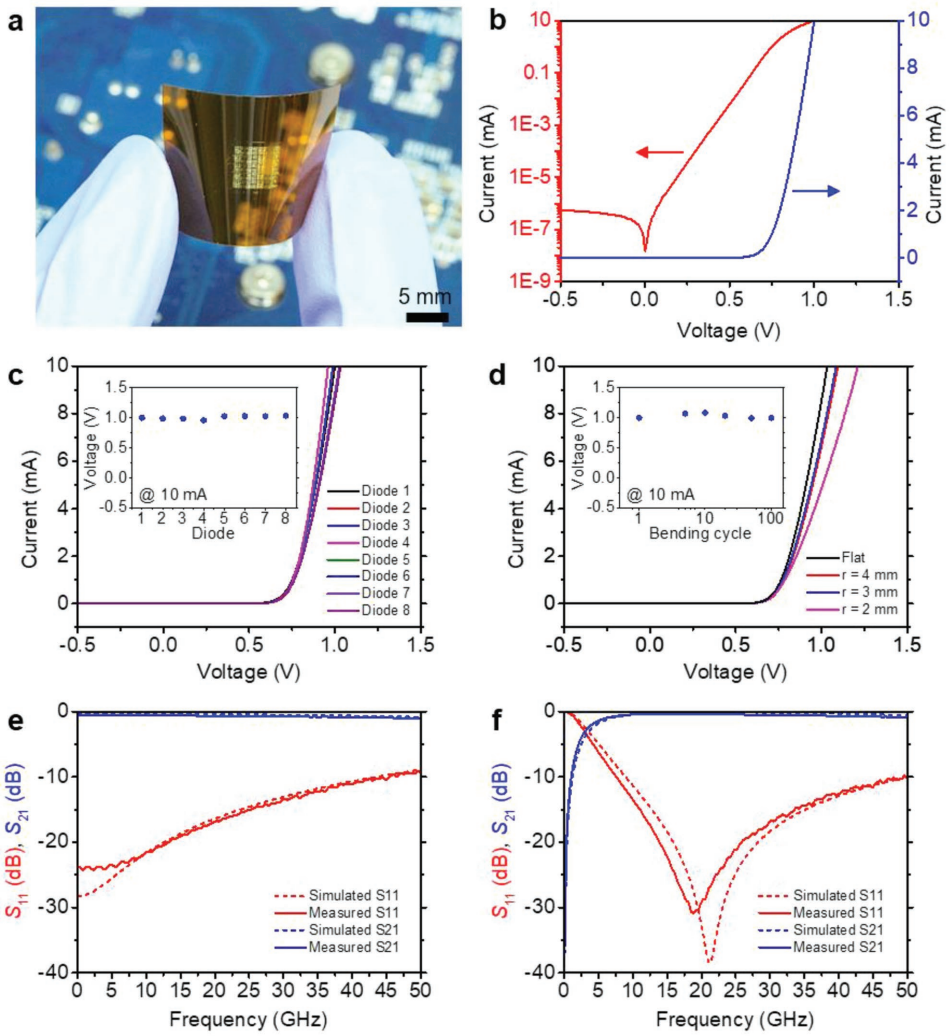

Figure 3. DC and RF analysis of the GaAs-based Schottky diode after release and printed onto a polyimide substrate. a) Photograph image of Schottky diodes printed onto a polyimide substrate. b) Current versus voltage plot of the printed Schottky diode on polyimide substrate. The red curve shows the logarithmic scale and the blue curve shows the linear scale. c) Current versus voltage linear plot of eight Schottky diodes. Inset shows the measured voltage plotted for each diode at forward current of 10 mA. d) Current versus voltage linear plot of a Schottky diode measured at different bending conditions (flat and radius of 4, 3, and 2 mm). Inset shows the measured voltage plotted for the diode after 1, 5, 10, 20, 50, and 100 bending cycles. e) Measured S_{11} (red) and S_{21} (blue) plotted against frequency under a forward current bias of 10 mA. Dotted curves show the simulation results. f) Measured S_{11} (red) and S_{21} (blue) plotted against frequency under a reverse voltage bias of –0.5 V. Dotted curves show the simulation results.

shown in Figure 4b. The capacitors used for this circuit were adapted from our previously demonstrated report on flexible passive devices, which presented high-performance inductors and capacitors operable up to X-band frequencies (≈10 GHz).[36] RF power was supplied using a high-frequency sweep oscillator and RF plug-in system via an RF ground–signal–ground (G–S–G) probe, and the DC output voltage was measured using an oscilloscope with a 10 Ω load via DC probes, as shown in Figure 4c. Efficiency trend plotted against different levels of input power reveals the RF-to-DC conversion capability at gigahertz frequencies (Figure 4d). With 20.19 dBm input power at 4 GHz, the rectifier based on printed diodes demonstrated maximum efficiency of 36.4%. The performance of the rectifier at different frequency levels was evaluated by plotting the output power levels against frequency with input power fixed at 10 dBm as shown in Figure 4e. The levels of efficiency can be manipulated and maximized by choosing the optimized load resistance and capacitance for different levels of frequency. The fabricated rectifier demonstrated stable operation under bending states, as presented in Figure 4f. Measured under different bending conditions (flat and radius of 38.5, 28.5, and 21.0 mm) at 5 GHz, the rectifier performed within rectification tolerance of 3.5%, 6.0%, and 8.5% for input power levels of 10, 15, and 20 dBm, respectively. The rectifier presented in this work can be utilized for many printed electronics applications, such as wireless power-harvesting circuits for wearable and implantable electronics. This also confirms the feasibility of our releasable diodes in an RF-integrated circuit operable at gigahertz frequencies.

In summary, the fabrication of high-performance releasable GaAs-based Schottky diodes capable of operating at microwave frequencies was presented. Protective anchors patterned using

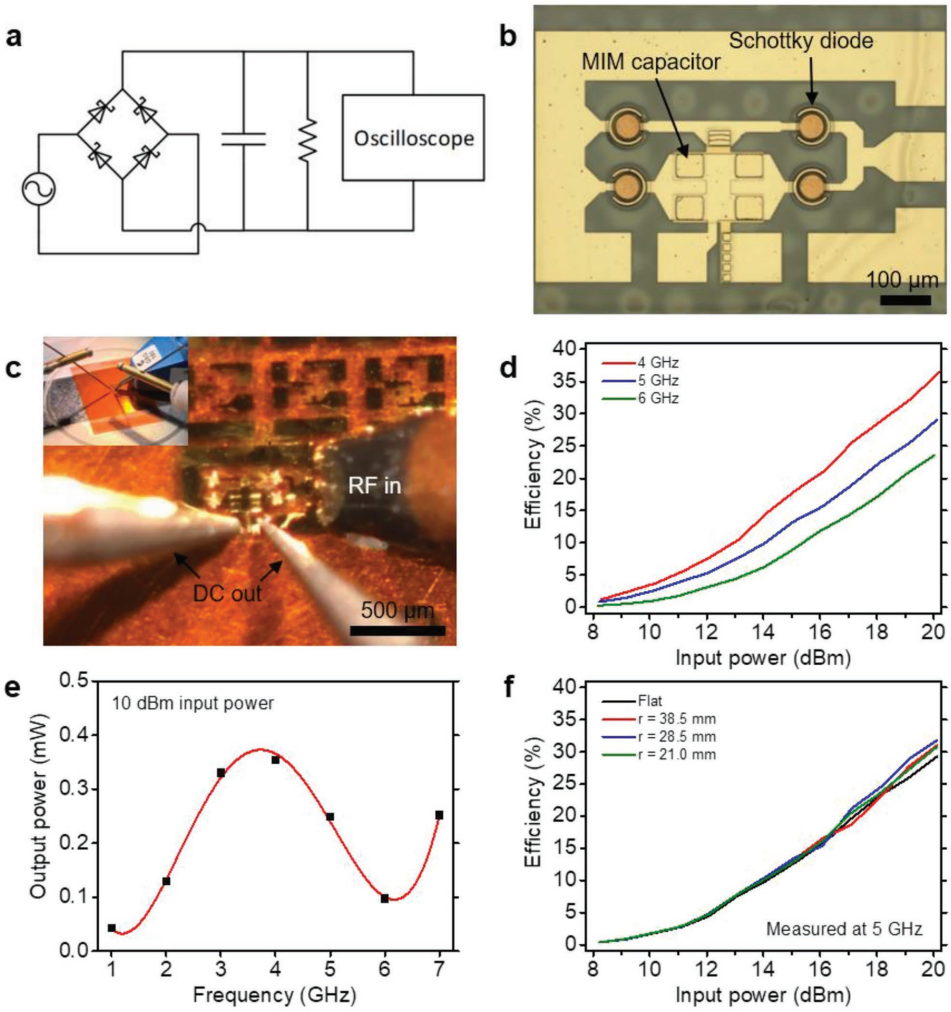

Figure 4. High-frequency full wave bridge rectifier built using releasable GaAs-based Schottky diodes. a) Circuit diagram of the full bridge rectifier using four Schottky diodes. b) Optical microscopy image of the full bridge rectifier. Schottky diodes were integrated with metal–insulator–metal capacitors into a microwave circuit. c) Photograph image of the rectifier during measurement. Input RF power was supplied via a coplanar waveguide probe and DC measurements were measured via two DC probes. Inset image shows the probe configurations. d) Efficiency curves plotted against RF input powers of 4, 5, and 6 GHz. Efficiency was calculated with measured DC output voltages through a 10 Ω load. e) DC output power measured under RF input power of 10 dBm against increasing frequencies with 1 GHz increments. Curve fitting provides rectification trend against frequency. f) Efficiency plotted against RF input power measured at 5 GHz under different bending conditions (flat and radius of 38.5, 28.5, and 21.0 mm).

photoresist allowed the etching of the sacrificial layer under the entire batch. This also created breakable bridges that released an individual diode during the pick-up process using an elastomer micro-stamp. The design and method for fabricating releasable diodes demonstrated in this work may further be configured for other electronic devices such as different types of transistors and diodes, passive components, and optoelectronics devices. Most importantly, fabrication schemes should focus on producing a large array of devices that have uniform performance parameters, with long storage times. Also, releasable fully formed devices using other high-performance III–V compound materials can be interesting towards utilizing the material's performance strength depending on applications. For example, power electronics in printed formats may benefit from releasable gallium nitride-based transistors, in which the wide bandgap allows the handling of high power. Developing a library of such devices for all types of electronic devices would provide high flexibility for circuit designers, where they can simply pick up a device of interest and print onto a targeted substrate in a sequential manner. This not only creates hybrid material combinations of devices on nearly any type of substrate, but also significantly reduces material cost and design efforts.

Experimental Section

Fabrication of GaAs-Based Releasable Schottky Diodes: The fabrication of the releasable diodes began with conventional plasma etching and deposition processes, followed by patterning of the photoresist-based protective anchors. To fabricate diodes on the rigid wafer, 800 nm thick hard mask of SiO_2 in circular shapes was deposited via a lift-off process, followed by deep plasma etching of the n^- GaAs layer to reach n^+ GaAs layer. Layers of metals were

deposited on the circular patterns (n^- GaAs) for anode formation and on the etched n^+ GaAs for cathode formation. First, cathode metal (Pd/Ge/Au = 30/40/200 nm) was deposited via a lift-off process and the sample was annealed at 450 °C for 30 s in ambient forming gas (H_2/N_2 = 5/95%) in a rapid thermal annealing (RTA) system for ohmic contact formation. A Schottky metal (Ti/Pt/Au = 10/30/200 nm) was deposited on an n^- GaAs layer for anode contact, followed by an inductively couple plasma (ICP)-reactive ion plasma etching (RIE)-based isolation process to etch away the excess n^+ GaAs layer and the exposed AlAs layer. Protective anchors were patterned by spin casting a thick (≈7.0 µm) photoresist layer (Megaposit SPR220; Rohm and Haas Electronic Materials) at 4000 rpm for 30 s, soft baked at 110 °C for 120 s, exposed to ultraviolet light at a dose of 500 mJ cm^{-2}, developed (MF-24A) for 120 s, and hard baked at 110 °C for 10 min. The AlAs sacrificial layer was undercut-etched using diluted HF (1:100 by deionized water: 49% HF) for 3 h.

Micro-Stamp Preparation: A pattern of negative photoresist (SU-8 50; Microchem, 100 µm) on a Si substrate was prepared for PDMS (Sylgard 184; Dow Corning, 10:1 mixture of pre-polymer to curing agent) molding of a 100 × 100 μm^2 elastomer micro-stamp for selective transfer printing of the devices.

Pick-Up and Transfer of Schottky Diode for Flexible Electronics: Preparation and fabrication of ultrathin polyimide-based flexible diode were done on a separate substrate. On a Si substrate, a thin layer of sacrificial polymer based on polymethyl methacrylate (950 PMMA A2; Microchem, 60 nm) was spin casted, followed by hard baking at 180 °C for 3 min. A thin sheet of polyimide was spin casted at 5500 rpm for 60 s on the top, followed by soft bake at 80 °C for 25 s to create adhesion. Using a micro-stamp mounted on a modified mask aligner, a Schottky diode was transfer printed on the polyimide adhesive and hard baked at 130 °C for 3 min. A quick spray of acetone removed the protective anchor on the device, but left the polyimide undamaged. Rectifier fabrication followed the same procedures described above with the addition of MIM capacitor fabrication. To insert MIM capacitors, the bottom metal layer was deposited (Ti/Au = 10/300 nm), followed by the deposition of the dielectric layer (TiO_2 = 200 nm) and top metal layer (Ti/Au = 10/300 nm) via lift-off processes. Another thin sheet of polyimide was spin casted, followed by soft bake at 150 °C for 5 min and hard bake at 300 °C for 1 h in a vacuum oven. Copper (100 nm) was deposited using an electron-beam evaporator with a lift-off process to serve as a hard mask to open via holes for the device contacts (both diodes and MIM capacitors), followed by RIE (CF_4/O_2 = 2/40 sccm, pressure = 300 mTorr, power = 200 W) of polyimide and wet etching of the copper mask. G–S–G RF pads (Ti/Cu/Ti/Au = 10/800/10/200 nm) were deposited via a lift-off process for DC and RF characterization of the device.

Supporting Information

Supporting Information is available from the Wiley Online Library or from the author.

Acknowledgements

Y.H.J. and H.Z. contributed equally to this work. This work was supported by the Air Force Office of Scientific Research (AFOSR): Presidential Early Career Award in Science & Engineering (PECASE) grant # FA9550-09-1-0482. The program manager was Dr. Gernot Pomrenke. Yei Hwan Jung was a Howard Hughes Medical Institute International Student Research Fellow. Y.H.J. and T.K. were supported by the Basic Science Research Program (NRF-2018R1D1A1B07048988 and NRF-2017R1D1A1B03033089, respectively) through the National Research Foundation of Korea funded by the Ministry of Science, ICT and Future Planning.

Conflict of Interest

The authors declare no conflict of interest.

Keywords

bridge rectifiers, flexible electronics, gallium arsenide, Schottky diodes, super high-frequency

Received: October 30, 2018
Published online:

[1] D.-H. Kim, J.-H. Ahn, W. M. Choi, H.-S. Kim, T.-H. Kim, J. Song, Y. Y. Huang, Z. Liu, C. Lu, J. A. Rogers, *Science* **2008**, *320*, 507.
[2] J. Yoon, S. Jo, I. S. Chun, I. Jung, H.-S. Kim, M. Meitl, E. Menard, X. Li, J. J. Coleman, U. Paik, J. A. Rogers, *Nature* **2010**, *465*, 329.
[3] H. Ko, K. Takei, R. Kapadia, S. Chuang, H. Fang, P. W. Leu, K. Ganapathi, E. Plis, H. S. Kim, S.-Y. Chen, M. Madsen, A. C. Ford, Y.-L. Chueh, S. Krishna, S. Salahuddin, A. Javey, *Nature* **2010**, *468*, 286.
[4] A. M. Hussain, M. M. Hussain, *Adv. Mater.* **2016**, *28*, 4219.
[5] R. J. Baker, *CMOS: Circuit Design, Layout, and Simulation*, Wiley-IEEE Press, Piscataway, NJ **2011**.
[6] Y. H. Jung, H. Zhang, S. J. Cho, Z. Ma, *IEEE Trans. Electron Devices* **2017**, *64*, 1881.
[7] L. Sun, G. Qin, J.-H. Seo, G. K. Celler, W. Zhou, Z. Ma, *Small* **2010**, *6*, 2553.
[8] K. Zhang, J.-H. Seo, W. Zhou, Z. Ma, *J. Phys. D: Appl. Phys.* **2012**, *45*, 143001.
[9] A. Carlson, A. M. Bowen, Y. Huang, R. G. Nuzzo, J. A. Rogers, *Adv. Mater.* **2012**, *24*, 5284.
[10] H.-J. Chung, T.-I. Kim, H.-S. Kim, S. A. Wells, S. Jo, N. Ahmed, Y. H. Jung, S. M. Won, C. A. Bower, J. A. Rogers, *Adv. Funct. Mater.* **2011**, *21*, 3029.
[11] T.-I. Kim, Y. H. Jung, H.-J. Chung, K. J. Yu, N. Ahmed, C. J. Corcoran, J. S. Park, S. H. Jin, J. A. Rogers, *Appl. Phys. Lett.* **2013**, *102*, 182104.
[12] W. Zhang, X. Zhang, C. Lu, Y. Wang, Y. Deng, *J. Phys. Chem. C* **2012**, *116*, 9227.
[13] N. Matsuhisa, H. Sakamoto, T. Yokota, P. Zalar, A. Reuveny, S. Lee, T. Someya, *Adv. Electron. Mater.* **2016**, *2*, 1600259.
[14] J. Zhang, Y. Li, B. Zhang, H. Wang, Q. Xin, A. Song, *Nat. Commun.* **2015**, *6*, 7561.
[15] N. Sani, M. Robertsson, P. Cooper, X. Wang, M. Svensson, P. A. Ersman, P. Norberg, M. Nilsson, D. Nilsson, X. Liu, H. Hesselbom, L. Akesso, M. Fahlman, X. Crispin, I. Engquist, M. Berggren, G. Gustafsson, *Proc. Natl. Acad. Sci. U. S. A.* **2014**, *111*, 11943.
[16] D. Im, H. Moon, M. Shin, J. Kim, S. Yoo, *Adv. Mater.* **2011**, *23*, 644.
[17] H. Kleemann, S. Schumann, U. Jorges, F. Ellinger, K. Leo, B. Lussem, *Org. Electron.* **2012**, *13*, 1114.
[18] J. Semple, D. G. Georgiadou, G. Wyatt-Moon, G. Gelinck, T. D. Anthopoulos, *Semicond. Sci. Technol.* **2017**, *32*, 123002.
[19] G. Qin, H.-C. Yuan, G. K. Celler, W. Zhou, Z. Ma, *J. Phys. D: Appl. Phys.* **2009**, *42*, 234006.
[20] G. Qin, H.-C. Yuan, Y. Qin, J.-H. Seo, Y. Wang, J. Ma, Z. Ma, *IEEE Electron Device Lett.* **2013**, *34*, 160.
[21] Y. H. Jung, T.-H. Chang, H. Zhang, C. Yao, Q. Zheng, V. W. Yang, H. Mi, M. Kim, S. J. Cho, D.-W. Park, H. Jiang, J. Lee, Y. Qiu, W. Zhou, Z. Cai, S. Gong, Z. Ma, *Nat. Commun.* **2015**, *6*, 7170.
[22] C.-W. Cheng, K.-T. Shiu, N. Li, S.-J. Han, L. Shi, D. K. Sadana, *Nat. Commun.* **2013**, *4*, 1577.

[23] K. Chen, R. Kapadia, A. Harker, S. Desai, J. S. Kang, S. Chuang, M. Tosun, C. M. Sutter-Fella, M. Tsang, Y. Zeng, D. Kiriya, J. Hazra, S. R. Madhvapathy, M. Hettick, Y.-Z. Chen, J. Mastandrea, M. Amani, S. Cabrini, Y.-L. Chueh, J. W. Ager III, D. C. Chrzan, A. Javey, *Nat. Commun.* **2016**, *7*, 10502.
[24] N. R. Glavin, K. D. Chabak, E. R. Heller, E. A. Moore, T. A. Prusnick, B. Maruyama, D. E. Walker, D. L. Dorsey, Q. Paduano, M. Snure, *Adv. Mater.* **2017**, *29*, 1701838.
[25] S. M. Sze, J. C. Irvin, *Solid-State Electron.* **1968**, *11*, 599.
[26] J. A. Del Alamo, *Nature* **2011**, *479*, 317.
[27] A. G. Baca, C. I. H. Ashby, *Fabrication of GaAs Devices*, IET, London **2005**.
[28] R.-H. Kim, S. Kim, Y. M. Song, H. Jeong, T.-I. Kim, J. Lee, X. Li, K. D. Choquette, J. A. Rogers, *Small* **2012**, *8*, 3123.
[29] Y. Yang, Y. Hwang, H. A. Cho, J.-H. Song, S.-J. Park, J. A. Rogers, H. C. Ko, *Small* **2011**, *7*, 484.
[30] S. Kim, J. Wu, A. Carlson, S. H. Jin, A. Kovalsky, P. Glass, Z. Liu, N. Ahmed, S. L. Elgan, W. Chen, *Proc. Natl. Acad. Sci. U. S. A.* **2010**, *107*, 17095.
[31] T.-I. Kim, Y. H. Jung, J. Song, D. Kim, Y. Li, H.-S. Kim, I. S. Song, J. J. Wierer, H. A. Pao, Y. Huang, *Small* **2012**, *8*, 1643.
[32] J.-K. Chang, H. Fang, C. A. Bower, E. Song, X. Yu, J. A. Rogers, *Proc. Natl. Acad. Sci. U. S. A.* **2017**, *114*, E5522.
[33] H.-S. Kim, E. Brueckner, J. Song, Y. Li, S. Kim, C. Lu, J. Sulkin, K. Choquette, Y. Huang, R. G. Nuzzo, J. A. Rogers, *Proc. Natl. Acad. Sci. U. S. A.* **2011**, *108*, 10072.
[34] W. C. B. Peatman, T. W. Crowe, *Int. J. Infrared Millimeter Waves* **1990**, *11*, 355.
[35] K.-W. Chung, Z. Wang, J. C. Costa, F. Williamson, P. P. Ruden, M. I. Nathan, *Appl. Phys. Lett.* **1991**, *59*, 1191.
[36] S. J. Cho, Y. H. Jung, Z. Ma, *IEEE J. Electron Devices Soc.* **2015**, *3*, 435.

